Collapse Study of a Pair Thin-Walled Prismatic Column Subjected to Oblique Loads

P. Hosseini-Tehrani[1,*] and S. Pirmohammad[2]

[1] Associate professor, [2] Phd student, School of Railway engineering, Iran University of Science and Technology, Tehran, Iran.

[*] hosseini_t@iust.ac.ir

Abstract

In the design of vehicle structures for crashworthiness there is a need for rigid subsystems that guarantee an undeformable survival cell for the passengers and deformable subsystems able to efficiently dissipate the kinetic energy. The front rails are the main deformable components dissipating energy in a frontal impact, which is the most dangerous crash situation. In frontal impact these rails have the greatest influence on vehicle crash performance. In this work study of different cross sections of the front rails under full frontal crash with different inclination angle of barrier considering two connected or two separated rails is carried out.

The present paper deals with the collapse simulation of two extruded polygonal section columns made of aluminum alloy which are separated or are connected with a nearly rigid bumper and, are subjected to oblique loads. Oblique load conditions in numerical simulations are applied by means of impacting a declined rigid wall on the tubes with no friction. The explicit finite element code LS-DYNA is used to simulate the crash behavior of polygonal section columns which are undergoing both axial and bending collapses situations. In order to validate LS-DYNA results the collapse procedure of square columns is successfully simulated and the obtained numerical results are compared with actual available experimental data. Mean crush loads and permanent displacements correspond to load angles have been investigated considering columns with square, hexagonal and, octagonal cross sections. It is shown that a pair of octagonal cross section connected columns has better characteristics from the point of view of crashworthiness under oblique load condition and connection between two rails dominates bending mode of deformation and reduces crashworthiness capability of front end of vehicle.

Keyword: *oblique loads, polygonal section column, crashworthiness, two connected column.*

1. INTRODUCTION

An increased emphasis is currently being placed on crashworthiness as a structural design requirement for occupant carrying vehicles. The goal of this effort is to design vehicles that can minimize the dynamic forces experienced by occupants during a crash event while at the same time maintaining them in a survivable structural envelope. To accomplish this goal it is necessary to evaluate the dynamic crush behavior of the vehicle structure in specific crash situations.

In applications such as vehicles, weight is a critical factor and must be minimized. Saving in weight using lightweight materials such as aluminum can lead to increased fuel economy and reduction in pollution. Aluminum alloys stand out as attractive material for body constriction being about one third lighter than steel but possessing comparable strength to weight ratio as steel. Aluminum also has superior corrosion-resistance and recyclability when comparing to mild or high strength steel. Usage of aluminum would, however, undoubtedly have a negative impact on cost; although it may be possible to meet the cost objectives by using extruded members, optimizing design by using computer-aided engineering, and minimizing expenses related to manufacturing

Crashworthy component in the form of thin-walled circular cylinder and frusta were firstly examined showing a proper and stable crash mode [1]. However, from applicability point of view, this solution met difficulties, mainly associated with mounting to other automobile structures. In this manner, due to practicality considerations, the use of stamped sheet metal members was selected in the fabrication of crashworthy components.

From the lightening and crashworthiness point of view an aluminum space frame is considered as a very promising type of car body structure, gaining increasing popularity for its high weight efficiency [2]. Another merit of the aluminum space frame is that almost every arbitrary cross-section can be produced by the extrusion process. In this regard extruded members are superior to the thin-walled structures made by unitizing sheet metal by spot-welding or bonding. For example, Honda uses complex hexagonal extruded cross-section members for the

front side rail of its new hybrid passenger car, Insight [3].

The primary collapses of thin-walled columns are axial and bending collapses, which have been studied from analytical, numerical and empirical points of view. Analytical studies of axial collapses have dealt with the mean crush load of square columns [4], rectangular columns [5, 6] and hat-type section columns [7, 8]. The results of these studies give simple and closed-form solutions of mean crush loads. The first comprehensive experimental study of the deep bending collapse of the rectangular column was made by Kecman [9]. He proposed simple failure mechanisms involving stationary and moving hinge lines. Wallentowitz and Adam [10] performed experiments on the hat-type section column under oblique loads and insisted on the need for such studies.

The objective of this paper is to investigate the crush behavior of thin-walled polygonal section columns subjected to oblique loads. Two connected and two separated columns are with different cross sections are studied and the effects of connection between columns and cross section are discussed. In this paper an optimization study is performed that involves the validation and suitability of dynamic impact numerical simulations to predict the permanent axial displacement, mean dynamic force and deformation characteristics of aluminum extruded tubes with different polygonal sections.

The commercial finite element program LS-DYNA that offers non-linear dynamic simulation capabilities is used in this study. Initially, the numerical results were compared against experimental data to verify the validity of the finite element model and material properties. The experimental data used to validate the initial numerical results are those of Langseth, Hopperstad, and Berstad [11- 14].

2. FORMULATION OF THE PROBLEM AND FINITE ELEMENT MODELING

The first structure which is considered in this study is a thin-walled extruded tube with square cross section that is modeled with varying wall thickness ranging from 1.80 to 2.5 mm. This square tube is used for comparing the LS-DYNA results with available experimental results. In order to find the best cross section against the oblique loading five different section configurations, square, hexagonal, octagonal,

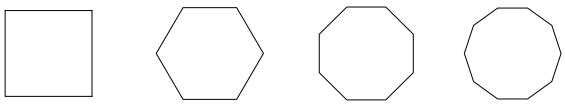

Fig. 1. Corresponding section of extruded tubes modeled.

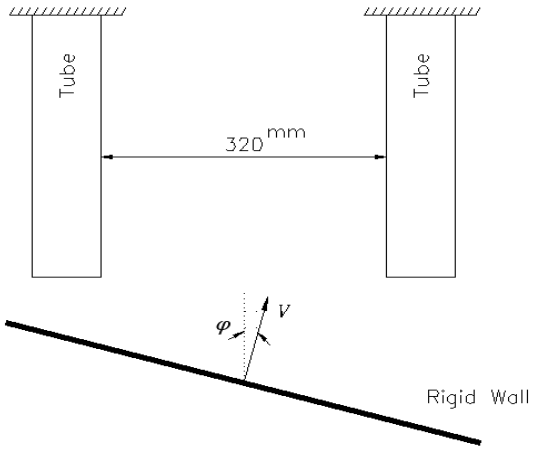

Fig. 2. Boundary condition for two separated rail under oblique loading.

and decagonal are considered for extruded tubes. The wall thickness and the cross section area of all tubes in this step are the same and equal to 2.5mm and 773 mm^2 respectively (fig. 1). All the extruded tubes and bumper are modeled using Belytschko-Tsay four-node shell elements with nine integration points through the thickness and one integration point in the element plane with the optimal mesh density for all the models being in the order of 4*4 mm. The boundary constraints for validation step is fixed at lower end and the top end is attached to a rigid body member modeled using shell elements. The rigid body member is modeled with one degree of freedom and that being translation along direction of velocity shown in figs. 2 and 3. The impact velocities are similar to those described in the experimental data [11] and are incorporated into the model by defining nodal velocities to the rigid body elements.

The boundary conditions for comparing the response of two separated and two connected rails are shown in fig. 2 and 3, as it is seen two separated rail are modeled as two tubes that are fixed at one end and are free to move in any direction without rotation (fig. 2). Fig. 3 shows the two connected rail with a nearly rigid bumper that is modeled as a strip (508^{mm} x104^{mm} x7^{mm}). The strip is made of steel and its material

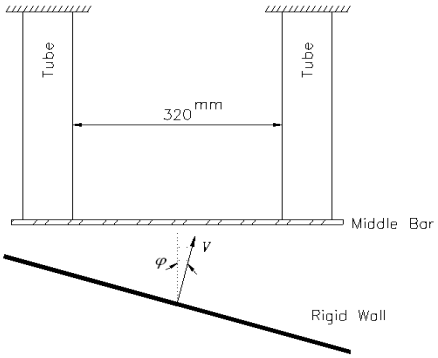

Fig. 3. Boundary condition for two connected rail under oblique loading.

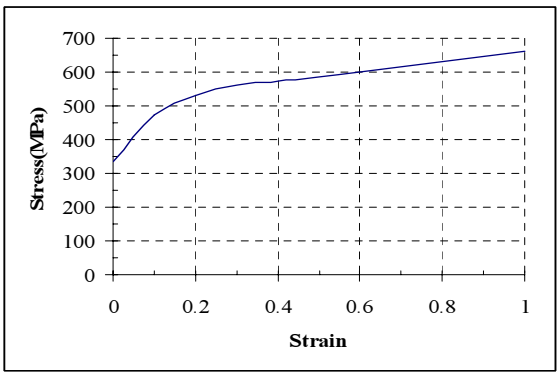

Fig. 4. stress strain curve for considered steel.

properties are as follow: $\rho = 7800\frac{Kg}{m^3}$, $E = 207000MPa$, $\sigma_0 = 335.5MPa$, the stress strain behavior of bumper's material is shown in fig. 4. The velocity of rigid wall is for all cases 13.2 m/sec and the angle between vertical axis and orthogonal line to the rigid wall varies between 0 to 30 degrees. The rigid body member is modeled with one degree of freedom and that being translation along the vertical axis (z-axis) which coincides with the direction of impact (figs. 5, 6).

All the tubes are modeled with 5168 elements and 5236 nodes, the strip is modeled with 2400 elements and 2541 nodes the simulated total impact mass being constant at 55.9 kg [11] for all single tubes which is the same considered weight for experimental test [11], and 111.8 kg for all the LS-DYNA models

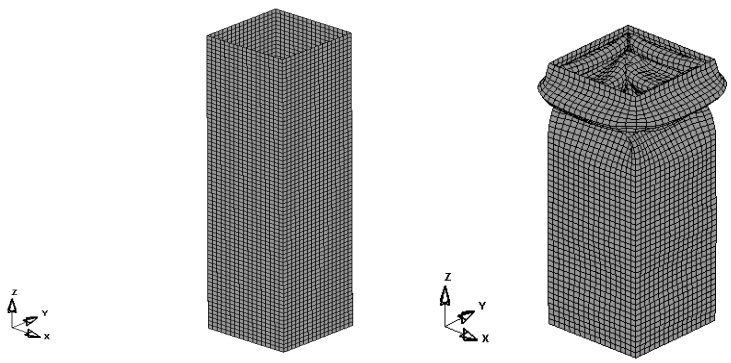

Fig. 5. Finite element models of square cross section tube before and after deformation.

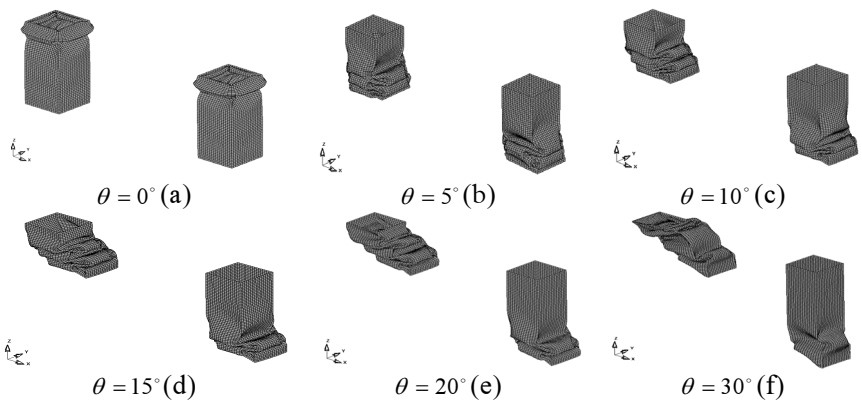

Fig. 6. Deformations of two separated square cross sectional tubes.

Table 1. True stress- strain data for aluminum alloy AA6060-T4 based on the uniaxial test for 2.5 mm wall thickness.

Plastic strain	0	0.002	0.025	0.05	0.075	0.1	0.15	0.175
Stress (Mpa)	75	82	116	140	150	162	164	168

Table 2. True stress- strain data for aluminum alloy AA6060-T4 based on the uniaxial test for 2 mm wall thickness.

Plastic strain	0	0.002	0.025	0.05	0.075	0.1	0.15	0.18
Stress (Mpa)	66	76	124	146	156	158	164	167

Table 3. True stress- strain data for aluminum alloy AA6060-T4 based on the uniaxial test for 1.8 mm wall thickness.

Plastic strain	0	0.002	0.025	0.05	0.075	0.1	0.15	0.175
Stress (Mpa)	56	71	126.5	143.5	146.5	152.5	156	158

configurations of double tubes. In addition, to facilitate the study in forming comparative assessments from the numerical results, it was decided to introduce additional geometric constraints which specified that all of the LS-DYNA models have equal cross section areas and thicknesses. The length of the extruded tube for all of the model configurations was 310 mm.

The "single surface" type of contact interface was selected to simulate the deformation of the specimen walls. This contact type uses nodal normal projections and prevents elements from penetrating the wall surfaces during the collapsing of the tube which is dominated by dynamic progressive buckling that manifests itself by the formation of various folds (lobes).

The material properties of aluminum alloy AA6060-T4 based on the uniaxial true stress-strain behavior of the material and wall thickness are shown in tables 1-3.

3. NUMERICAL SIMULATION RESULTS

In the first phase of the investigation, the LS-DYNA simulation results were validated with experimental dynamic impact test data published by both Langseth and Hopperstad [11]. These authors have published extensive experimental data pertaining to the static and dynamic axial crushing of aluminum square tube extrusions. They have also established with reasonable accuracy the material properties pertaining to those of the aluminum alloy AA6060 T4 and T6 test specimens using standard tensile testing. Also, in conjunction with the work done by Opheim [12], it was discovered that no significant differences exist in the behavior of the materials, regardless of

Table 3. True stress- strain data for aluminum alloy AA6060-T4 based on the uniaxial test for 1.8 mm wall thickness.

Specimen test	$t(mm)$	$A(mm^2)$	$V(ms^{-1})$	$\delta_p(mm)$	$P_{md}(KN)$
1.8-1	1.80	581	10.28	117	24.6
1.8-2	1.81	581	10.17	129	21.8
1.8-3	1.80	581	8.47	87	22.5
2.0-4	1.96	625	11.64	126	29.3
2.0-5	1.96	625	14.06	184	29.7
2.0-6	1.95	625	9.45	82	29.7
2.5-7	2.44	773	13.20	117	40.6
2.5-8	2.44	773	11.10	73	46.0
2.5-9	2.45	773	15.60	158	41.9

Table 5. LS-DYNA simulation results for square extrusion tube and comparison with experimental results

LS-DYNA model	t (mm)	A (mm^2)	V(ms^{-1})	$\delta_p\,(mm)$	$\Delta\delta(\%)$	$P_{md}\,(KN)$	$\Delta P_{md}\,(\%)$
1.8-1	1.8	581	10.28	121	-3.42	23.8	+3.3
1.8-2	1.8	581	10.17	125	+3.10	22.2	-1.83
1.8-3	1.8	581	8.47	90	-3.45	23.1	-2.67
2.0-4	2.0	625	11.64	131	-3.97	29.7	-1.37
2.0-5	2.0	625	14.06	189	-2.72	30.4	-2.36
2.0-6	2.0	625	9.45	84	-2.44	30.8	-3.70
2.5-7	2.5	773	13.20	115	+1.71	42.1	-3.69
2.5-8	2.5	773	11.10	76	-4.11	45.6	+0.87
2.5-9	2.5	773	15.60	165	-4.43	41.7	+0.48
Average					-2.19		-1.22

tension or compression loading.

To gauge the validity of the LS-DYNA numerical simulations in predicting the average mean crushing force (P_{md}) and deformation behavior (δ_P) of an axially impacted member, it is decided to arbitrarily select experimentally tested specimens that are representative of the spectrum of parameters tested (i.e. wall thickness, impact velocity, and deformation mode) with only the specimens fabricated from aluminum alloy AA6060-T4 being the focus of this investigation. The selected specimens whose dynamic experimental test data are to be predicted by LS-DYNA numerical simulation are presented in Table 4. Table 5 presents the corresponding LS-DYNA numerical simulation results for the square extrusion tubes and the error percentage of these results compared with the experimental results.

As shown in Table 5, the LS-DYNA numerical simulation results are able to predict the permanent axial displacement (δ_P) with an upper bound absolute error percentage of 4.43% when compared to the experimental results whereas the mean dynamic force (P_{md}) is predicted with an upper bound absolute percentage error of 3.7%. Also as significant, is that the post-buckling deformation behavior predicted by LS-DYNA is very similar to that described by Langseth and Hopperstad [11] in their published experimental results, i.e. symmetric mode lobe deformations which are shown in fig. 5. The good correlation achieved between the computational numerical and experimental results allowed the second phase of the research study to be conducted with a reasonable degree of confidence. Furthermore, the square section specimens are used as a baseline to help assess the energy absorbing performance of the more complex hexagonal, octagonal, and decagonal sections.

The structures which are considered in this section are eight pairs of thin-walled extruded tubes with square, hexagonal, octagonal, and decagonal cross section. All the extruded tubes were modeled similar to section 2. In other words, for all the tube configurations one end is fixed and the other end, in separated pair, is free to move in any direction without rotation and in connected pair the other end is fixed on the bumper which is simplified as a strip in this study.

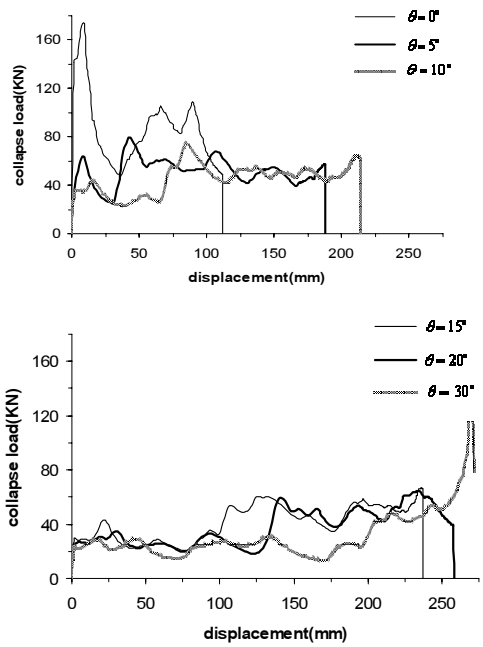

Fig. 7. Rigid wall force versus displacement at the end of the two separated square tubes.

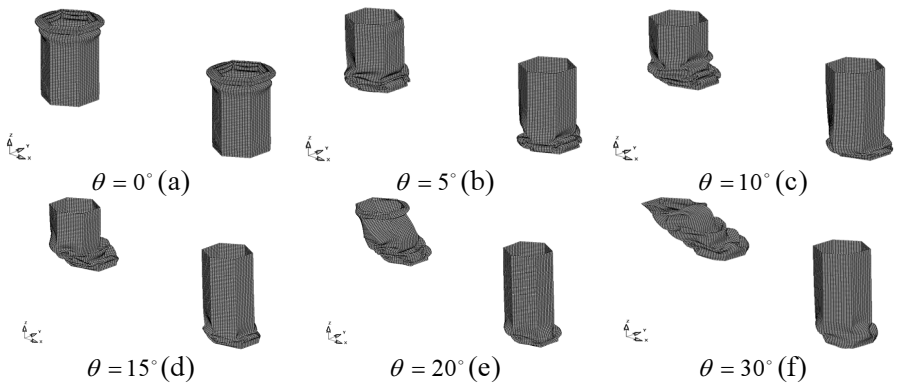

Fig. 8. Deformations of two separated hexagonal cross sectional tubes.

An inclined rigid wall impacts on the tube and sticks the end of the tube or the bumper. The velocity of rigid wall is 13.2 m/sec (figs. 2 and 3). The rigid body member was modeled with one degree of freedom and that being translation along direction of velocity. The sectional area, A, would be constant for a given wall thickness, "t" equal to 2.5 (mm) and is considered equal to 773 (mm^2). The length of the extruded tube for all of the model configurations is 310 mm. The material properties of aluminum alloy AA6060-T4 based on the uniaxial true stress-strain behavior of the material are used for the tubes in this section.

Figs. 6- 13 show deformed shapes and variation of collapse load versus displacement of tubes under different inclination angles of rigid wall considering various cross-sections for separated tubes. In figs 14-21 the same results are driven for connected tubes. In figs. 6 and 7 where the inclination angle of rigid wall is 30 degree the collapse mode of one square tube causes the rigid wall tobe pushed against the fixed boundary and could not continue the movement.

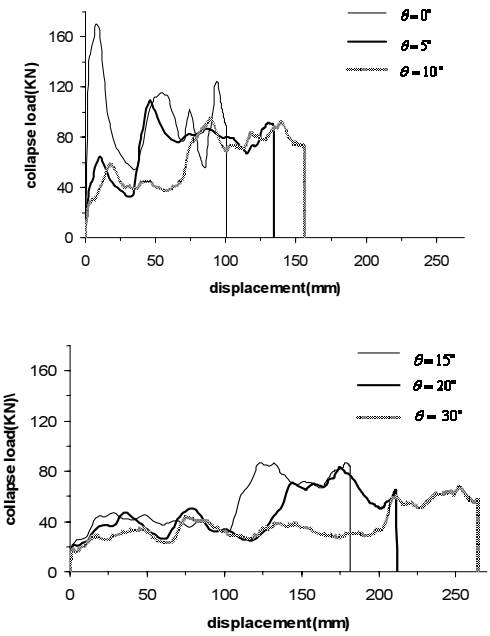

Fig. 9. Rigid wall force versus displacement at the end of the two separated hexagonal tubes.

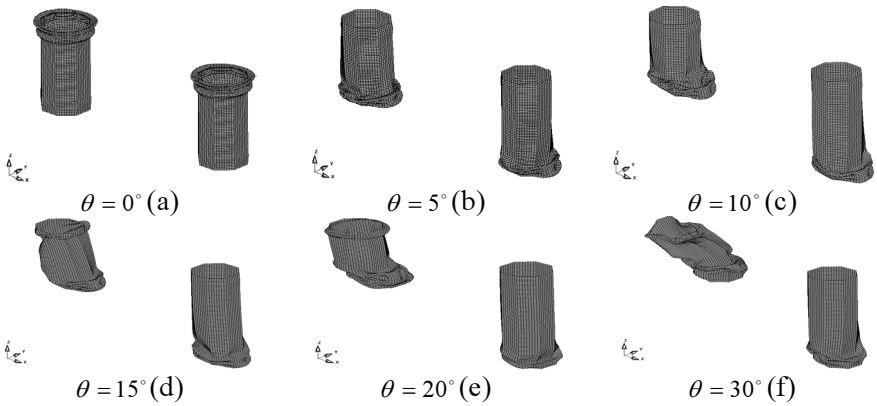

Fig. 10. Deformations of two separated octagonal cross sectional tubes.

Table 6. LS-DYNA simulation results for different cross-section pairs of separated tubes.

Results of numerical simulations	$\theta(\deg ree)$	$\delta_p(mm)$	$P_{md}(kN)$
Square			
	0	112	87
	5	188	51.8
	10	214	45.6
	15	237	41
	20	258	37.8
	30	-	-
Hexagonal			
	0	101	96.4
	5	134	72.6
	10	157	62
	15	182	53.6
	20	212	46
	30	264	36.8
Octagonal			
	0	97	100.4
	5	131	74.4
	10	162	60.2
	15	180	54.2
	20	196	49.6
	30	281	34.6
Decagonal			
	0	97	100.4
	5	133	73.2
	10	161	60.4
	15	174	56
	20	202	48.2
	30	262	37.2

Table 7. LS-DYNA simulation results for different cross-section pairs of connected tubes with a bumper.

Results of numerical simulations	$\theta(\deg ree)$	$\delta_p(mm)$	$P_{md}(kN)$
Square			
	0	108	90.2
	5	191	51.0
	10	218	44.7
	15	240	40.6
	20	277	35.2
	30	296	32.9
Hexagonal			
	0	98	99.4
	5	135	72.2
	10	156	62.4
	15	182	53.5
	20	204	47.8
	30	275	35.4
Octagonal			
	0	95	102.5
	5	133	73.2
	10	152	64.1
	15	177	55.0
	20	205	47.5
	30	268	36.3
Decagonal			
	0	96	101.5
	5	131	74.4
	10	156	62.4
	15	181	53.8
	20	207	47.1
	30	265	36.7

Therefore in this case the result may not be completed.

Tables 6 and 7 show the LS-DYNA numerical simulation results that are permanent displacement (δ_p) and the mean dynamic force (Pmd) for different angle of inclination of the rigid wall considering various cross sections. Tables 8 and 9 show the comparison of the

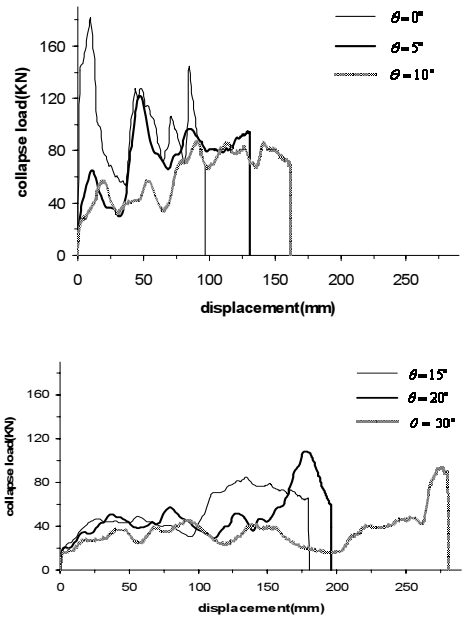

Fig. 11. Rigid wall force versus displacement at the end of the two separated octagonal tubes.

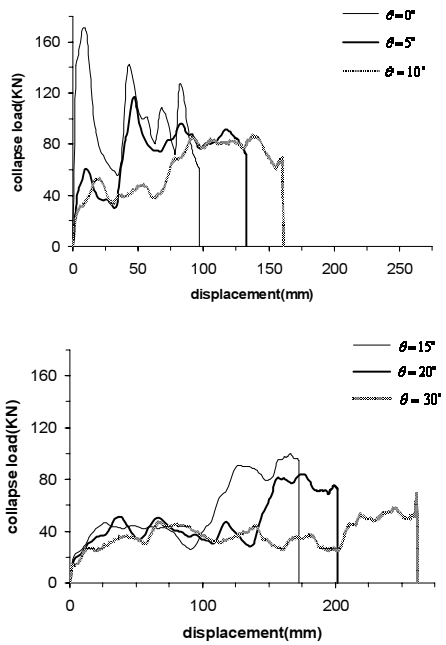

Fig. 13. Rigid wall force versus displacement at the end of the two separated decagonal tubes.

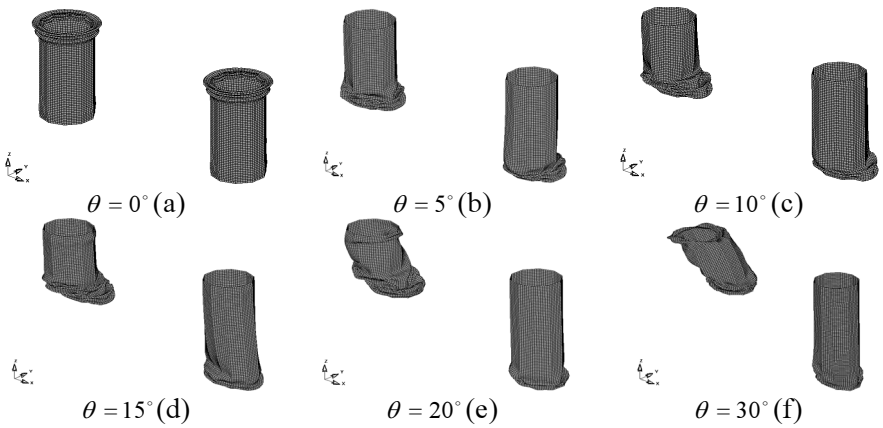

Fig. 12. Deformations of two separated decagonal cross sectional tubes.

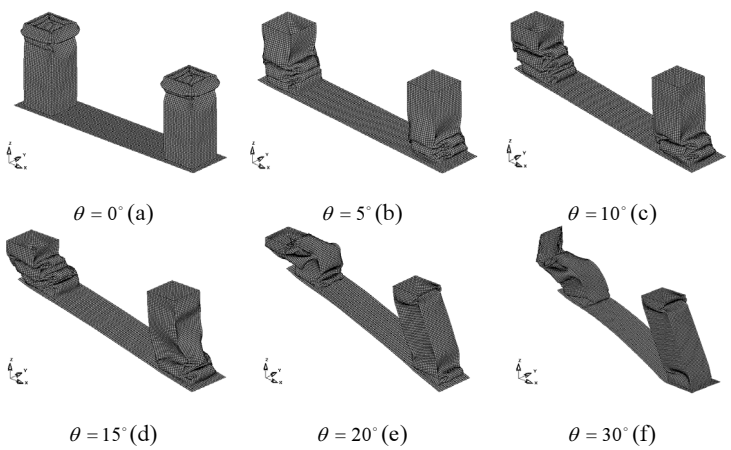

Fig. 14. Deformations of two separated square cross sectional tubes.

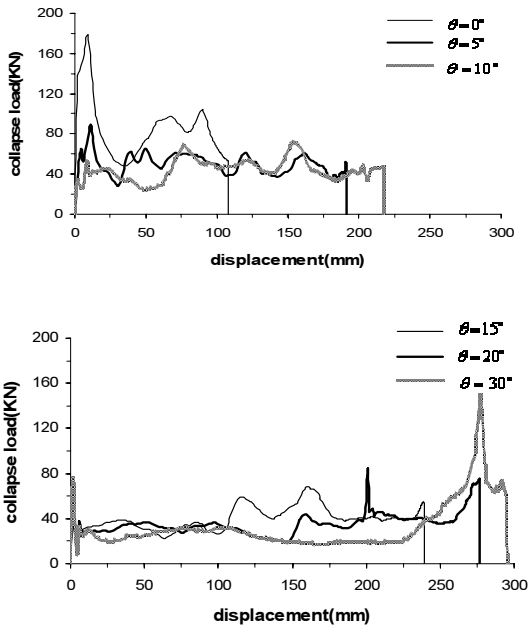

Fig. 15. Rigid wall force versus displacement at the end of the two connected square tubes.

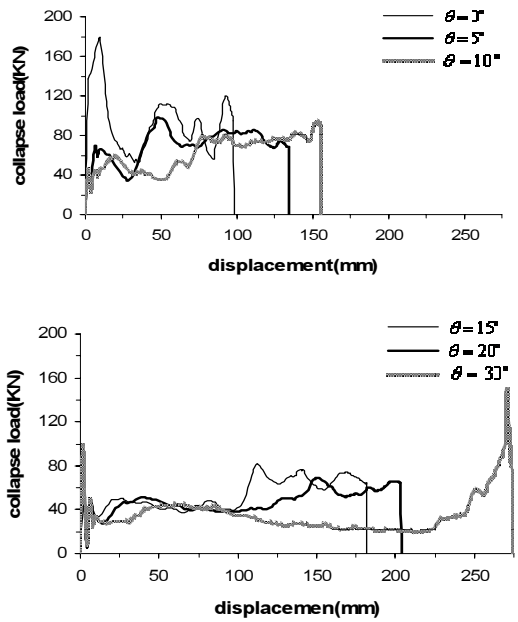

Fig. 17. Rigid wall force versus displacement at the end of the two connected hexagonal tubes.

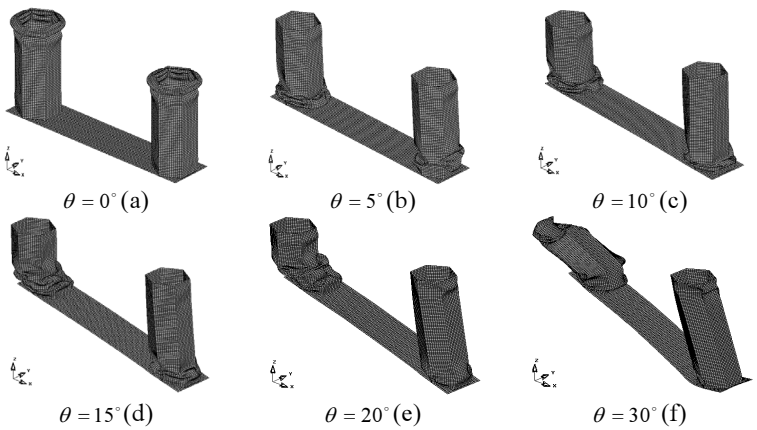

Fig. 16. Deformations of two separated hexagonal cross sectional tubes.

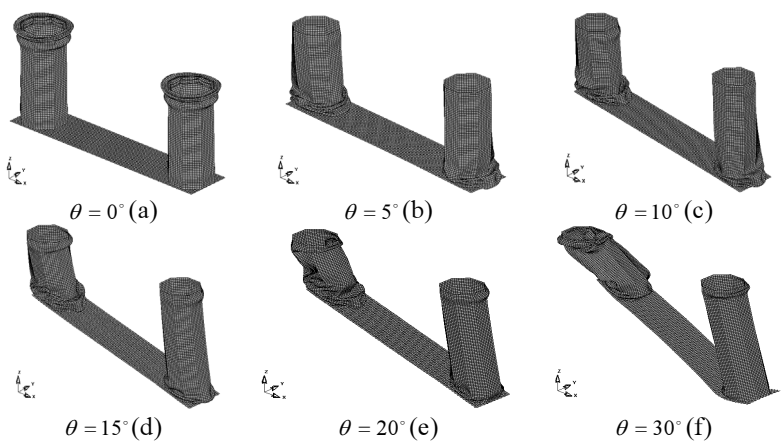

Fig. 18. Deformations of two separated octagonal cross sectional tubes.

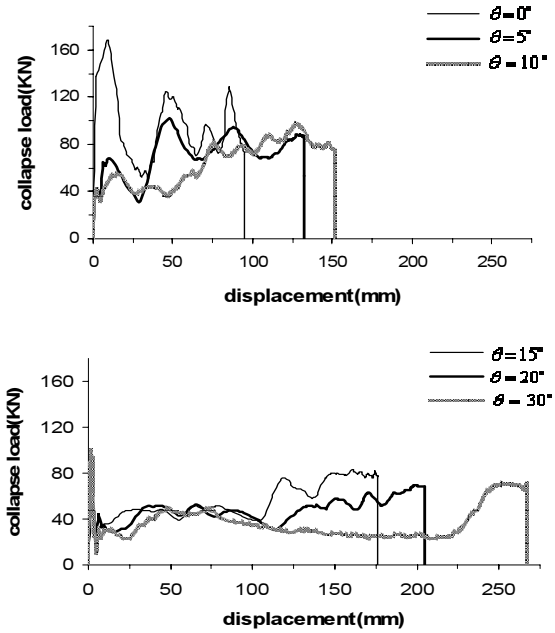

Fig. 19. Rigid wall force versus displacement at the end of the two connected octagonal tubes.

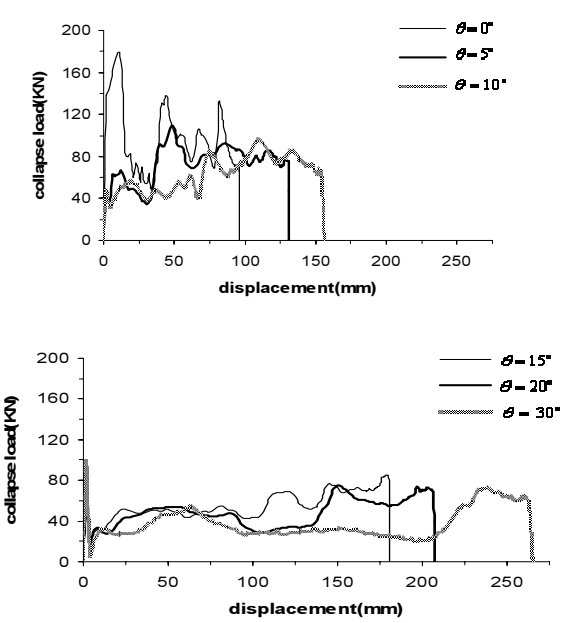

Fig. 21. Rigid wall force versus displacement at the end of the two connected decagonal tubes.

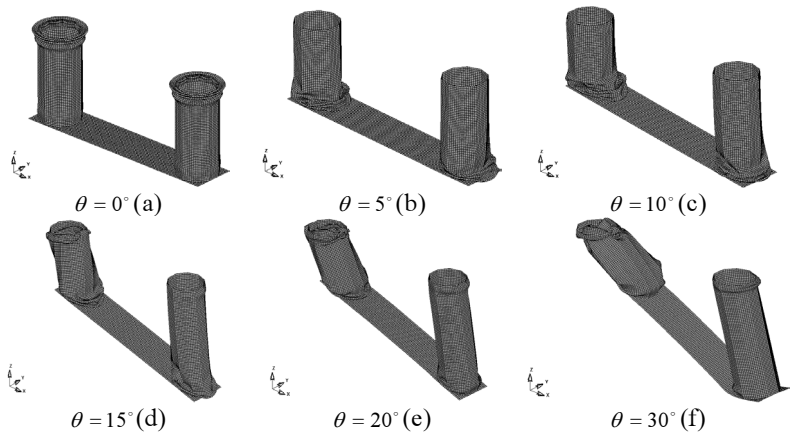

Fig. 20. Deformations of two separated decagonal cross sectional tubes.

result of different cross-sections with the square cross-section.

In figs 7, 9, 11 and 13, it is seen where the inclination angle is not zero no dramatic rise in force occur at the beginning of the deformation for separated tubes especially when the inclination angle is more than 15 degree. Besides in figs. 9, 11 and 13 two distinct areas may be recognized in which the difference between mean force and intentness force is not remarkable. Therefore it may be concluded that at the beginning of the deformation or where the impact load is not sever, deceleration is not very high and if there is more need for energy absorption the capability of energy absorbing may be rise as the mean force become higher. In figs 6, 8, 10 and 12 no distortion or folding is observed near the fix end of the right hand tubes so in the case of two separated tubes acceleration variation and damaged area are limited comparing with two connected tubes.

In figs 14 – 21, dramatic changes in curves that represent the force response of two connected tubes are observed and opposite of the case of two separated tubes the folding area is not limited and damage is spread all over the length of the two tubes.

From tables 8 and 9, it is seen that octagonal cross section for most inclination angles shows the biggest

Table 6. LS-DYNA simulation results for different cross-section pairs of separated tubes.

results	$\theta(\deg ree)$	$\Delta\delta_p(\%)$	$\Delta P_{md}(\%)$
Hexagonal section tubes			
	0	-9.8	10.8
	5	-28.7	40.2
	10	-26.6	36.0
	15	-23.2	30.7
	20	-17.8	21.7
	30	-	-
average		-21.2	27.9
Octagonal section tubes			
	0	-13.4	15.4
	5	-30.3	43.6
	10	-24.3	32.0
	15	-24.1	32.2
	20	-24.0	31.2
	30	-	-
average		-23.2	30.9
Decagonal section tubes			
	0	-13.4	15.4
	5	-29.3	41.3
	10	-24.8	۳۲.۵
	15	-26.6	36.6
	20	-21.7	27.5
	30	-	-
average		-23.1	30.7

Table 7. LS-DYNA simulation results for different cross-section pairs of connected tubes with a bumper.

results	$\theta(\deg ree)$	$\Delta\delta_p(\%)$	$\Delta P_{md}(\%)$
Hexagonal section tubes			
	0	-9.3	10.2
	5	-29.3	41.6
	10	-28.4	39.6
	15	-24.2	31.8
	20	-26.3	35.8
	30	-7.1	7.6
average		-20.8	27.8
Octagonal section tubes			
	0	-12.0	13.6
	5	-30.4	43.5
	10	-30.3	43.4
	15	-26.3	35.5
	20	-26.0	34.9
	30	-9.6	10.3
average		-22.4	30.2
Decagonal section tubes			
	0	-11.1	12.5
	5	-31.4	45.9
	10	-28.4	39.6
	15	-24.6	32.5
	20	-25.3	33.8
	30	-10.5	11.5
average		-21.8	29.3

mean dynamic force while its average permanent displacement is the shortest, besides manufacturing process of octagonal tubes is less complicated than decagonal tubes. As a result, octagonal cross section may be the best choice from the points of view of energy absorption characteristic and price in both cases (separated and connected tubes).

4. CONCLUSIONS

In this task the crushing behavior of a separated or connected pairs of thin-walled polygonal columns

subjected to oblique loads is studied. Using a number of numerical models the following important results are drawn.

1. Considering a pair of separated thin walled tube that is subjected to oblique loads, it has been demonstrated that the mean crush load may be divided in two parts: the first is a region where the mean force is low and consequently deceleration and injury are not remarkable, and the second is a region where the mean force is high and the energy absorption is significant. It is shown that the first region will be extended if the inclination of rigid wall increases. This fact is related to the mechanism in that the two columns take part in deformation. As the inclination angle increases the bending mode will be the dominating mode of deformation in the left hand tube as well as the right hand tube participation in energy absorption will be lesser. It is seen that the number of walls of cross section does not affect on this phenomenon. As a result with the aid of this finding a proper design procedure may be done to eliminate the disadvantages of each region.
2. In the case of passenger transportation systems, it is also necessary to ensure that the passengers can tolerate an impact. In other words, the magnitude of the peak in the crushing force-axial displacement characteristics which determine the deceleration amount and the value of Head Injury Criterion must be tolerable to the passenger. For investigation of the maximum amount of crushing force study of variation of crushing force versus displacement may be done. It is seen that for a given impact velocity while the cross-sectional area of the studied tubes are the same, the peak of the crushing force occurs when the load angle is zero and this peak is nearly the same for all studied cross sections in this task. It is seen that in the case of two separated columns for other inclination angles no dramatic changes on force distribution occur while for two connected tubes several jumps in force response may be seen. As a result a separated pair of tube is preferable from the point of view of passenger safety.
3. Despite the above results which show any remarkable preferences among different cross sections, it is seen that octagonal cross section for most inclination angles shows the biggest mean dynamic force and square cross section for all inclination angles provides the smallest mean dynamic force, while the average permanent displacement of octagonal cross section is the shortest and the opposite result is observed for square cross section. As a result, octagonal cross section may show better energy absorption characteristic with minor damage under oblique loading as well as under axial loading.
4. It is seen that in the case of two separated tubes the folding area is limited to the front end of the tubes while for two connected tubes damage is spread all over the length of the two tubes. Therefore from the point of view of repairmen two separated tube is more suitable.
5. Although the two connected tubes are heavier and more expensive in comparison with two separated tubes they do not show better characteristic for energy absorption. As a result connection between the front rails in a vehicle has no positive effect from the point of view of crashworthiness and is not recommended.

REFERENCES

[1] Jones N., Structural Impact. Printed by: Cambridge University Press, paperback edition 1977.

[2] Chung T-E, Lee Y-R, Kim C-S, Kim H-S, Design of aluminum space frame for crashworthiness improvement. SAE paper no. 960167, 1996.

[3] Fukuo K., Fujimura A., Saito M., Tsunoda K., Takiguchi S.,Development of the ultra-low-fuel-consumption hybrid car-insight. JSAE Review 2001; 22:95-103.

[4] Abramowicz, W., Jones N. Dynamic axial crushing of square tubes. Int J Impact Eng 1984;2(2):179-208.

[5] Mahmood HF, Paluszky A. Design of thin walled column for crash energy management-their strength and mode of collapse. In: proc Fourth Int conf on vehicle structural Mechanics, Detroit (MI), November 1981:7-18

[6] Wierzbicki T, Abramowicz W. On the crushing

mechanics of thin-walled structures. J Appl Mech 1983;50:727-34

[7] Tani M, Funahasi A. Energy absorption by the plastic deformation of body structural members. SAE Technical Paper 780368. Dearborn (MI): Society of Automotive Engineers, 1978.

[8] Okubo Y, Akamatsu T, Shirasawa K. Mean crushing strength of closed-hat section members. SAE Technical Paper 740040. Dearborn (MI): Society of Automotive Engineers, 1974.

[9] Kecman D. Bending collapse of rectangular and square section tubes. Int J Mech Sci 1983; 25(9/10):623-36.

[10] Wallentowitz H, Adam H. Predicting the crashworthiness of vehicle structures made by Lightweight design materials and innovative joining methods. Int J crashworthiness 1996;1(2):163-80.

[11] Langseth M, Hopperstad O. Static and dynamic axial crushing of square thin-walled aluminum extrusions. Int J Impact Eng 1996;18(7/8):949-68.

[12] Opheim B. Bending of thin-walled extrusions' Doctoral Thesis. Trondheim: Norwegian University of Science and Technology; 1996.

[13] Langseth M, Hopperstad O. Berstad T. Square aluminum tubes subjected to oblique loading. Int J Impact Eng 2003;28:1077-106.

[14] Langseth M, Hopperstad O. Berstad T. Crashworthiness of aluminum extrusions: validation of numerical simulation, effect of mass ratio and impact velocity. Int J Impact Eng 1999;22:829-54